Oxygen Evolution at Platinum Electrodes in Alkaline Solutions

II. Mechanism of the Reaction

V. I. Birss*

Department of Chemistry, University of Calgary, Calgary, Alberta, T2N 1N4, Canada

A. Damjanovic and P. G. Hudson

Allied Corporation, Corporate Research and Development Center, Morristown, New Jersey, 07960

ABSTRACT

Kinetic data of the oxygen evolution reaction at Pt electrodes in alkaline solutions have shown two types of behavior, a Tafel slope of 60 mV/decade of current density at low applied current densities and a slope of 120 mV/decade at high current densities. At low current densities, and rate of the reaction was found to be independent of the thickness of the underlying Pt oxide film, while the electrode potential has a −120 mV dependence on solution pH. At high current densities, the rate is strongly dependent on film thickness and exhibits a −180 mV dependence on pH. A mechanism of the oxygen evolution reaction which is consistent with this data is presented. It involves a rate-determining first electron transfer step at high current densities. At low current densities, the chemical step following the now rapid first electron transfer step is rate limiting. The −180 mV pH dependence observed at high current densities implies a fractional reaction order of 3/2 with respect to the OH^- ion. This has been explained in terms of a dual barrier model of the metal oxide film/solution interface. According to this model, the rates across each barrier are pH dependent. The fractional reaction order is due to the existence of these two dependences and is primarily related to the dependence of the potential difference across the outer Helmholtz layer on pH.

In a previous paper (1), it was shown that, depending on the applied current density, two types of kinetics characterize the oxygen evolution reaction at Pt electrodes in alkaline solutions. At low current densities, the Tafel slope is 60 mV/decade, while at high current densities, it is 120 mV/decade. The classifications of "low" and "high" current densities reflect electrode behavior with different Tafel slopes.

In the low current density region, the rate of oxygen evolution was found to be independent of the pretreatment of the electrode and, therefore, of the thickness of the oxide film covering the Pt electrode surface. Also, the rate of the reaction was found to depend strongly on the pH of the solution, *i.e.*, $dE/d\ pH = -120$ mV. The empirical rate equation is, therefore, given by

$$i_l = k_l[OH^-]^2 \exp[FE/(RT)] \quad [1]$$

The subscript l refers to the low current density region. E is the potential of the Pt electrode with respect to a pH independent reference electrode, and k_l is the pre-exponential factor, which has been found to be independent of the oxide film thickness but dependent on the choice of the reference electrode.

In contrast to the kinetics at low current densities, the rate of oxygen evolution at high current densities exhibits a clear dependence on the electrode pretreatment and, hence, on the oxide film thickness. Also, at high currents, the rate of oxygen evolution depends even more strongly on pH than in the low current density region, *i.e.*, $dE/d\ pH = -180$ mV/pH unit. This dependence is unusual in electrode kinetics and leads to a fractional reaction order of 3/2 with respect to the OH^- ion concentration. The rate equation, therefore, is given by (1)

$$i_h = k_h[OH^-]^{3/2} \exp[FE/(2RT)] \quad [2]$$

The subscript h refers to high current density. The dependence of the rate of the O_2 evolution reaction on the film thickness at high currents is seen by the dependence of k_h on the film thickness.

In this paper, we discuss the kinetic data in relation to the recently proposed structure of the double layer at oxide covered Pt electrodes and also propose a mechanism for oxygen evolution in alkaline solutions which is consistent with the observed data in both the low and the high current regions and with the new views of the structure of the double layer.

Comparison of the kinetics at high current density in alkaline solutions with the kinetics in acid solutions.—The kinetics in the high current region, including the observed fractional reaction order of 3/2 with respect to OH^- ions, cannot be explained on the basis of a simple model of the structure of the double layer and in terms of the generally accepted concepts of electrode kinetics. According to an early analysis by Bockris (2), a reaction order of 3/2 would imply that ⅓ of an OH^- ion ends up in the final product of a reaction, having bypassed the rate-determining step (rds), while the other ⅔ has crossed the potential energy barrier associated with the rds. Also, this fractional reaction order cannot be accounted for in terms of Temkin adsorption kinetics because a Tafel slope of 120 mV/decade is not consistent with any rds under Temkin conditions and because coverage with adsorbed oxygen species at oxide covered Pt surfaces is very small (3).

It is shown below that a reaction order of 3/2 with respect to OH^- has the same origin as the fractional reaction order of −½ with respect to H_3O^+ ions, reported for the oxygen evolution reaction in acid solutions (4-7), and that both are related to the structure of the double layer and the distribution of the potential at the metal/metal oxide film/solution interfaces. As at high currents in alkaline solutions, the rate of oxygen evolution at all currents in acid solutions also depends critically on the thickness of the film (5, 7, 8). In order to facilitate understanding of the fractional reaction order in alkaline solutions and the dependences of the rate of oxygen evolution on film thickness, the nature of the parallel reactions of film growth and oxygen evolution should first be briefly discussed.

The exact relationship between Pt oxide film growth and the oxygen evolution reaction in acid solutions was studied in ring-disk electrode experiments (6, 7), in which a constant anodic current density, i, was first applied to an oxide free Pt disk electrode. Following the initial adsorption of oxygen species, a film forms upon the Pt substrate, while the potential increases linearly with time (Fig. 1). No oxygen could be detected at the ring up to a disk potential of about 1.5V. However, at a certain potential, which depends on i, oxygen began to evolve in a parallel process to film growth, and soon oxygen evolution became the predominant reaction. Then the potential continued to increase, but more slowly and nonlinearly with time and at a rate which decreased with time. In this nonlinear E-t region, the oxide film continued to grow slowly, while oxygen evolution was the predominant electrode reaction. This was determined (5, 6) by comparing the oxygen reduction current at the ring, which is proportional to the oxygen evolution current at the disk, with the current at the disk electrode, which is equal to the sum of the current due to O_2 evolution, i_{O_2}, and the current due to Pt oxide

* Electrochemical Society Active Member.

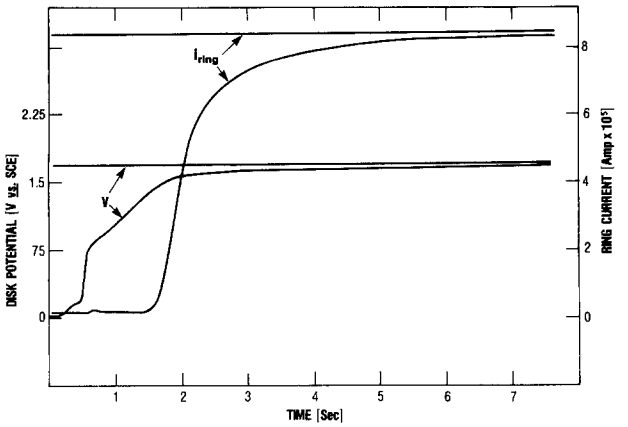

Fig. 1. Rotating ring-disk experiments. The changes of the ring current and the disk potential with time (0-7.5s and 7.5-15s are both shown) are indicated. $i_{disk} = 10^{-3}$ A/cm². Solution: 2N H_2SO_4.

growth, i_{og}. From the difference of $i - i_{O_2}$, i_{og} could then be obtained as a function of potential and time. The numerical integration of i_{og} over time gives the charge density equivalent to the Pt oxide film thickness.

With this approach, the high field Cabrera-Mott model of film growth, which is known to apply prior to the onset of oxygen evolution in both acid and alkaline solutions (3,9-14), could be tested for its validity in the case where O_2 evolution is the predominant reaction. If the film continued to grow according to the high field mechanism, even when O_2 evolution is the predominant reaction, then the equation

$$i_{og} = i_{og,o} \exp[(E - E_o)/(cq)] \quad [3]$$

which has been known to be valid in the linear E-t region where only Pt oxide growth occurs, must also hold in the nonlinear E-t region, in which O_2 evolution is the predominant reaction. In Eq. [3], $i_{og,o}$ can be considered as the exchange current density for Pt film growth, q is the charge density equivalent to the thickness of the oxide film, c is a constant which can be experimentally determined, and $E - E_o$ is the potential difference across the film and the inner Helmholtz layer (IHL) (3, 6, 7, 11-14). E_o is the potential in the inner Helmholtz plane (IHP) against the reference electrode [see Ref. (6, 7)]. By utilizing the values of $i_{og,o}$, c, and E_o, which were obtained from the Cabrera-Mott treatment of the data obtained in the linear E-t region, and the values for i_{og} obtained by the ring-disk experiment described above, the expected electrode potential in the nonlinear E-t region, E, was calculated from Eq. [3]. This calculated potential was then compared to the experimentally observed potential at the disk at the same charge density. A very close match was obtained between the calculated and observed potentials. This is illustrated in Fig. 2 for two current densities and two pH's.

This close match indicates that the same mechanism of Pt oxide growth applies at potentials prior to the occurrence of O_2 evolution as when O_2 evolution is the major reaction. Because of the applicability of Eq. [3] in both E/t regions, the model of the potential distribution across the film and the inner and outer Helmholtz layers, established in prior studies of Pt oxide growth, must also apply when O_2 evolution is the predominant reaction (7). According to this model, the potential difference across the outer Helmholtz layer (OHL), which is linearly related to E_o, is constant irrespective of the rate at which the oxide film grows and independent of its thickness. Consequently, E_o and, hence, the Galvani potential difference across the OHL, ${}^{OHP}\Delta^{IHP}\phi$, is independent of the rate at which oxygen is evolved. Here, OHP represents the outer Helmholtz plane. However, E_o has been found to vary with solution pH with respect to a pH independent reference electrode (cf., Fig. 2).

In Fig. 3, a model of the potential distribution at the metal/oxide film/solution interface is illustrated for two current densities and two pH's. The ring-disk experiments

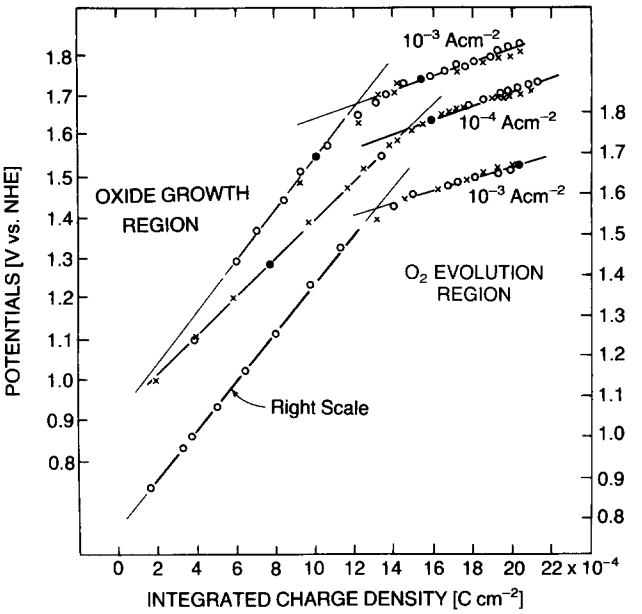

Fig. 2. Change of the disk potential with the integrated charge density. ○: observed potentials; x: calculated potentials using Eq. [3]. Two top lines, 2N H_2SO_4. Bottom line, 0.02N H_2SO_4.

and the comparison of the calculated and experimentally observed E/q relationships in acid solutions have shown that E_o decreases 60 mV as the pH increases by one unit in both E/q regions (cf., Fig. 2 and 3). Hence, the pH dependence of the oxygen evolution reaction in acid solutions, where water molecules are the reacting species in the rds, has been shown to be a direct consequence of the pH dependence of the potential difference across the OHL.

In contrast to E_o, the potential difference across the film and the IHL, $E - E_o$, is independent of the solution pH, although it varies with the applied current. Also, for the same i, $E - E_o$ changes as q, or the thickness of the film changes. It is evident from Fig. 2 that at any q during O_2 evolution, $E - E_o$ is given by (1, 7)

$$E - E_o = 2RT/\mathbf{F}\,[\ln(i/k_A) + mq] \quad [4]$$

Here m is the slope, dE/dq, in the second V-q region where O_2 evolution predominates and $i \sim i_{O_2}$. The constant, k_A, may be interpreted as the exchange current density for O_2 evolution extrapolated to zero film thickness (7).

The rds for oxygen evolution in acid solutions has been determined to be the first electron transfer step across the film and the IHL (6, 7). The true reaction order with respect to H_3O^+ ions with H_2O as the reacting species would then be zero. Although the process across the OHL is fast and independent of i, E_o decreases 60 mV as the pH increases

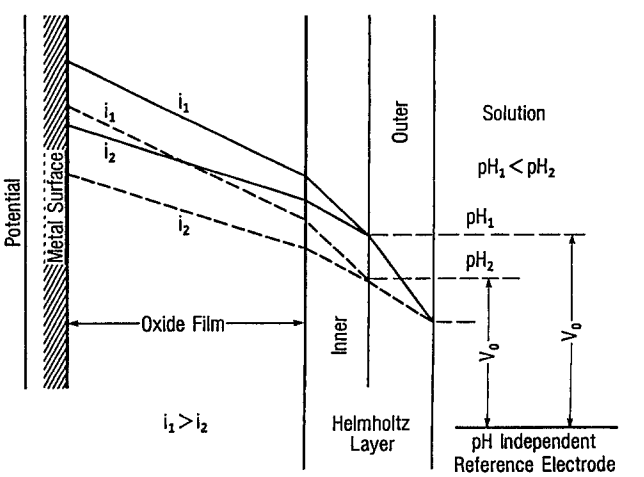

Fig. 3. Model of the dual barrier for O_2 evolution used in the present study.

one unit. In this model of two barriers in series, it is this dependence of E_o on pH which causes a $dE/d\ pH = -60$ mV and, hence, the observed fractional reaction order of $-\frac{1}{2}$ for O_2 evolution in acid solutions. This interpretation of the fractional reaction order can now be used to facilitate the understanding of the kinetics of O_2 evolution in alkaline solutions.

Dependence of the rate of oxygen evolution on pH at high current density.—Previous work in alkaline solutions (13, 14) has shown that prior to the onset of O_2 evolution, an oxide film grows at Pt, also according to the high field Cabrera-Mott law, *i.e.*, according to Eq. [3], although some kinetic parameters in acid and alkaline solutions differ. For example, $i_{o,og}$ is pH dependent in alkaline but not in acid solutions (10, 13). In order to analyze the observed pH dependence of O_2 evolution in alkaline solutions, the assumption is now made that the oxide film continues to grow according to the same mechanism during the O_2 evolution reaction as prior to it in alkaline solutions, as it did in acid solutions. It is also assumed that the observed hindrance of oxygen evolution in alkaline solutions by the presence of the underlying film can be represented by the same rate equation as is used for acid solutions.

Therefore, in the high current region in alkaline solutions, where the rate of O_2 evolution depends on film thickness, Eq. [2] can be re-expressed by assuming that k_h depends on film thickness, as was observed in acid solutions (Eq. [4]). The rate is then also proportional to exp $[-m\mathbf{F}q/(2RT)]$, *i.e.*,

$$i_h = b_h[OH^-]^{3/2} \exp[-m\mathbf{F}q/(2RT)] \exp[\mathbf{F}E/(2RT)] \quad [5]$$

In previous studies of film growth in alkaline solutions, at potentials prior to the onset of O_2 evolution, it was concluded that, as in acid solutions, the potential difference across the OHL is independent of i_{og} and film thickness, but it decreases 60 mV as pH increases one unit. Indeed, over the entire pH range, it was found that (3, 11, 14)

$$E_o = E_{o,pH=0} - 2.3RT/\mathbf{F}\ pH \quad [6]$$

E_o has the same significance as in Eq. [3], *i.e.*, it is the potential of the IHP with respect to a pH independent reference electrode. Although E_o and $E_{o,pH=0}$ are known only with respect to such an electrode, the change in E_o (with pH) is known. Consequently, E_o is said to provide a measure of the potential difference across the OHL. The effect of the diffuse double layer can be ignored in these concentrated solutions.

Although ring-disk electrode experiments to study these reactions in alkaline solutions have not been carried out, it is expected that when O_2 evolution becomes the predominant reaction at higher potentials, the Pt oxide film will continue to grow by the same mechanism as when only Pt oxide growth occurs at lower potentials. The potential drop across the OHL is then independent of the rate of O_2 evolution and the thickness of the oxide film, although it decreases 60 mV as pH increases one unit. Therefore, only the potential difference across the film and the IHL, $E - E_o$, which is independent of the choice of the reference electrode, determines the rate of oxygen evolution. For the first electron transfer step involving OH^- as the reactant, and replacing E in Eq. [5] by $(E - E_o)$ as the operative electrode potential (15), one obtains

$$\vec{i}_h = B_h[OH^-] \exp[-m\mathbf{F}q/(2RT)] \exp[\mathbf{F}(E - E_o)/(2RT)] \quad [7]$$

Equation [7] shows that, at high currents, the true reaction order with respect to OH^- is one. The additional dependence on pH, as seen by the fractional reaction order of 3/2 (Eq. [5]) for the overall reaction, arises only from the dependence of E_o on pH, according to Eq. [6].

In interpreting the film and film/solution interface as two barriers in series, one being the film and the IHL, and the other being the OHL, the rate of O_2 evolution at high currents and at a given pH is controlled by the electron transfer process across the film and IHL. For a constant film thickness, an increase in the potential difference across the film and IHL by 120 mV causes a 10-fold increase in the current for O_2 evolution. The process across the OHL and hence E_o, is independent of the rate of O_2 evolution.

Mechanism of oxygen evolution at high current density.—In view of the observed Tafel slope of 120 mV and the "true" reaction order of one with respect to OH^-, it is proposed that the rds of the O_2 evolution reaction at high currents is the first electron transfer step across the film and IHL. The reaction species is OH^- in the IHP, not H_2O molecules, as in acid solutions, *i.e.*

$$OH^-_{IHP} \rightarrow OH_{IHP} + e_M^- \quad [8]$$

A rapid equilibrium between OH^-_{IHP} and OH^-_{sol} exists, *i.e.*

$$OH^-_{IHP} \rightleftharpoons OH^-_{OHP} \rightleftharpoons OH^-_{sol} \quad [9]$$

Here, sol represents the bulk solution.

The overall rate equation for reaction [8] would then be given by

$$\vec{i}_h = k_h[OH^-]_{sol} \exp[\beta\mathbf{F}(E - E_o)/(RT)] \quad [10]$$

which is identical to rate Eq. [7] when $\beta = \frac{1}{2}$ and $k_h = B_h \exp[-m\mathbf{F}q/(2RT)]$.

A formal analogy may now be drawn between the dual barrier model, proposed for O_2 evolution, and the structure of the metal/solution interface in the presence of a diffuse double layer. The potential difference between the OHP and the bulk of solution in the case of the diffuse double layer is analogous in the dual barrier model to the potential difference across the OHL, assuming the absence of a diffuse layer in the latter. An equilibrium is established between the IHP and OHP and also between the OHP and the solution, in the dual barrier model, just as in the case of a diffuse double layer. As pointed out by Frumkin and discussed by others, *e.g.*, Delahay (16), the diffuse double layer affects the kinetics of an electrochemical reaction in two ways. First, the concentration of the reactants in the "pre-electrode plane," *i.e.*, the OHP in the diffuse double layer model, is different from the bulk concentration when the reactants are charged particles. Second, the "effective electrode potential" at the OHP is not $\phi_M - \phi_s$ but $\phi_M - \phi_2$. Here, ϕ_M and ϕ_2 are the inner potentials in the metal electrode and the OHP, respectively, and ϕ_s is the inner potential in the solution.

Following the analogy, in the dual barrier model, only the potential difference across the film and the IHL, $E - E_o = \phi_M - \phi_{IHP}$, affects the rate of O_2 evolution directly, and only the concentration of OH^- in the IHP (the pre-electrode plane in the DBM) should be considered in Eq. [10]. The concentration of a reacting ion, j, in a pre-electrode plane, *e.g.*, the OHP in the DDL model or the IHP in the dual barrier model, is related to the bulk concentration, *e.g.*, for the diffuse double layer model by (16)

$$C^j_{OHP} = C^j_{sol} \exp[-z\mathbf{F}(\phi_2 - \phi_{sol})/(RT)] \quad [11]$$

Here, z is the charge of the reacting ion and includes its sign. Although Eq. [11] may be valid for low concentrations of reactants and supporting electrolyte, *e.g.*, for concentrations less than $10^{-3}M$, this equation cannot be applied to high solution concentrations. For the dual barrier model, it predicts an OH^- concentration in the IHP which is excessively high as well as an impossibly high separation of charges across the OHL. Even if Eq. [11] were valid and the concentration of the reacting OH^- in solution were low, *e.g.*, less than $10^{-4}M$, any change in the concentration of OH^- ions in the IHP due to a change of the potential difference across the OHL, *e.g.*, due to pH changes, would be accompanied by a change in the ground level energy of OH^- in the IHP. This would, in turn, result in a change in the reaction activation energy, which will counteract the effect of the change of the OH^- concentration in the IHP on the rate of O_2 evolution. However, it should be pointed out that Eq. [11] represents only the change in the electrical energy when an ion is transferred from the bulk of solution to the OHP. Changes in the chemical energy, *e.g.*, chemical potentials, are not encompassed by Eq. [11] and, hence, the validity of the equation is questionable. In view of this qualification, it seems justifiable to consider that

$$[OH^-_{IHP}] \alpha [OH^-_{OHP}] \alpha [OH^-_{sol}] \quad [12]$$

so that, in Eq. [10], the OH^- concentration in the solution, rather than the OH^- concentration in the IHP, is used.

It should also be noted that although E_o decreases 60 mV as the pH increases by one unit, this does not necessarily imply that the Galvani potential difference across the OHL, $\phi_{IHP} - \phi_s$, changes 60 mV with each unit of pH. Consider a concentration cell consisting of two half-cells, each with a Pt electrode in an oxygen saturated solution of different pH. The cell potential difference is equal to the difference in the "absolute electrode potentials." Using the definition of the potentials suggested by Trasatti (17), the operative electrode potentials, $\Delta\phi$'s, are the same at both electrodes, and the observed difference in the cell potentials arises solely from the difference in the chemical potential of the electrodes in the different solutions, *i.e.*

$$\Delta E = \Delta\mu_e^s/e \qquad [13]$$

These chemical potentials can be expected to vary with the logarithm of the concentration of the reactants in these solutions. Consequently, the potential difference across the OHL of the working electrode would remain constant, independent of pH. In this case, Eq. [12] is unqualifiably correct. Indeed, there is evidence that the operative electrode potential of the RHE is independent of pH (18). To our knowledge, such a possibility has never been examined before in relation to electrode kinetics.

Mechanism at low current density.—Any interpretation of the kinetics of O_2 evolution in alkaline solutions in the low current region must be compatible with the reaction path and the model of the structure of the metal/solution interface proposed for the kinetics at high currents. It must also logically lead to the observed rate Eq. [1] and must be consistent with the observed independence of the O_2 evolution reaction at low currents on the thickness of the film. It must also account for the observed nonfractional dependence of the reaction rates on pH.

Formally, the observed Tafel slope of 60 mV and the pH dependence of −120 mV per pH unit, observed at low currents, would be consistent with the rds being a second, chemical step following a first rapid charge transfer step, *e.g.*

$$OH^- \underset{k_{-1}}{\overset{k_1}{\rightleftharpoons}} OH + e^- \qquad [14]$$

$$OH + OH^- \underset{k_2}{\overset{\text{rds}}{\rightleftharpoons}} \text{products } (e.g., O^- + H_2O) \qquad [15]$$

However, this path, (Eq. [14] and [15]), would yield the observed kinetic parameters only for a simple model of the double layer or when the potential difference across the entire interface determines the reaction rate. The reaction path with Eq. [15] as the rds is, therefore, not compatible with the proposed model and the kinetics in the high current region.

In view of the proposed model of the metal/solution interface and the mechanism of O_2 evolution at high currents, it is suggested now that at low currents, a chemical step following the rapid first electron transfer step is the rds. In anticipation of the results of this analysis, the rate of a chemical step without OH^- as the reactant in this step would be proportional to the concentration of OH_{IHP}, *i.e.*

$$\vec{i}_l = k_2[OH_{IHP}] \qquad [16]$$

By considering the first step (Eq. [14]) to now be in dynamic equilibrium and that the rate of [14], in both directions, will still depend on film thickness, as in Eq. [7], we can formulate

$$\vec{i}_h \sim k_{-1}[OH_{IHP}] \exp[-m\mathbf{F}q/(2RT)] \exp[-\mathbf{F}(E - E_o)/(2RT)] \qquad [17]$$

Then by equating $\vec{i}_h$ and $\overleftarrow{i}_h$, *i.e.*, [7] and [17], the $\exp[-m\mathbf{F}q/(2RT)]$ terms cancel out and

$$[OH_{IHP}] \alpha [OH^-_{sol}] \exp[\mathbf{F}(E - E_o)/(RT)] \qquad [18]$$

Therefore, from Eq. [16], the rate with a chemical step being the rds is given by

$$\vec{i}_l = k_l[OH^-_{sol}] \exp[\mathbf{F}(E - E_o)/(RT)] \qquad [19]$$

The "true" reaction order with respect to OH^- for the chemical step is one, but since E_o in Eq. [19] depends on pH, the apparent reaction order of two is obtained. Moreover, the rate is now independent of film thickness. Thus, Eq. [19] is now in agreement with the kinetic data of O_2 evolution observed in the low current density region and is compatible with the reaction path proposed for the kinetics in the high current density region and with the model of the metal/solution interface previously suggested.

Several chemical steps which satisfy the observed kinetic data and are consistent with Eq. [16] can now be suggested. For instance, the steps

$$OH_{IHP} + 2H_2O_{IHP} \rightarrow [H_2O_2^-{}_{IHP} + H_3O^+{}_{IHP}] \qquad [20]$$

or

$$OH_{IHP} + H_2O \rightarrow [O^-{}_{IHP} + H_3O^+] \qquad [21]$$

both formally satisfy the observed pH dependence. The intermediates in these steps are given only tentatively, as indicated by the square brackets. Any H_3O^+ in the IHP is either immediately neutralized by excess $OH^-{}_{IHP}$, or is rapidly transferred to the OHP, where it is neutralized by $OH^-{}_{OHP}$.

It should be noted that the chemical rds at low currents may actually involve the interaction of the OH species in the IHP with O or OH species already belonging to the film. Rozenthal and Veselovskii (19), using a tracer technique, have provided unique evidence that an oxygen species in the surface of the film participates directly in O_2 evolution. A reaction path in which oxygen atoms in the oxide surface participate in the process has also been proposed recently by Bockris and Otagawa (20) for lanthanum nickelate electrodes and was also suggested earlier for O_2 evolution at Ni oxide electrodes (21). At RuO_2 electrodes, reaction paths involving the direct participation of oxygen species in the oxide surface have also been suggested (22, 23). In all of these cases, the oxygen vacancies in the surface of the oxide are subsequently replenished in a fast parallel process, similar to that of film growth.

The experimental evidence from the studies of oxide growth at Pt have shown that Pt oxide films are poor electronic conductors, and that their properties do not change once oxygen begins and continues to evolve. The actual process of electron transfer across the film as required in the oxygen evolution reaction must then involve a quantum mechanical tunneling process through the film, which is expected to exhibit a dependence on the film thickness. This aspect of the mechanism should be addressed separately.

Manuscript submitted July 22, 1985; revised manuscript received March 19, 1986.

The University of Calgary assisted in meeting the publication costs of this article.

LIST OF SYMBOLS

b_h	pre-exponential factor of rate equation for oxygen evolution in high Tafel slope region
c	constant
C^j_{OHP}, C^j_{sol}	concentration of species j in OHP, or in solution bulk
E	potential
E_o	potential of inner Helmholtz plane *vs.* reference electrode
$\mathbf{F}$	Faraday constant
i	current density
$i_h(\vec{i}_h, \overleftarrow{i}_h)$	current density in high Tafel slope region (forward and reverse)
$i_l(\vec{i}_l, \overleftarrow{i}_l)$	current density in low Tafel slope region (forward and reverse)
i_{og}	current density due to oxide film growth
$i_{og,o}$	i_{og} at $E = E_o$; exchange current density for oxide film growth
i_{O_2}	current density due to oxygen evolution
IHL	inner Helmholtz layer
IHP	inner Helmholtz plane
j	species
k_l	pre-exponential factor of rate equation for oxygen evolution in low Tafel slope region
k_h	pre-exponential factor of rate equation for oxygen evolution in high Tafel slope region (including effect of oxide film)

k_A	exchange current density for oxygen evolution when oxide film thickness equals zero
k_1, k_{-1}, k_2	rate constants
m	slope of E/q plot for oxide film growth
OHL	outer Helmholtz layer
q	charge density equivalent to thickness of oxide film
rds	rate determining step
R	gas constant
T	temperature, K
z	charge of ion

Greek

β	symmetry factor
ϕ_m, ϕ_2, ϕ_s, ϕ_{IHP}	Galvani potential in metal, OHP, solution and IHP, respectively
${}^{OHP}\Delta^{IHP}\phi$	difference in Galvani potentials between OHP and IHP

REFERENCES

1. V. I. Birss and A. Damjanovic, Submitted to *This Journal.*
2. J. O'M. Bockris, in "Modern Aspects of Electrochemistry," Vol. 1, J. O'M. Bockris and B. E. Conway, Editors, p. 180, Academic Press, New York (1954).
3. K. J. Vetter and J. W. Schultze, *J. Electroanal. Chem.*, **34,** 131, 141 (1972).
4. T. Erdey-Gruz and O. Golopencza-Bajor, *Acta Chim. Hung.*, **34,** 281 (1962).
5. A. Damjanovic and B. Jovanovic, *This Journal,* **123,** 374 (1976).
6. V. I. Birss and A. Damjanovic, *ibid.*, **130,** 1694 (1983).
7. V. I. Birss and A. Damjanovic, *ibid.*, **130,** 1688 (1983).
8. J. W. Schultze and K. J. Vetter, *Electrochim. Acta, 18,* 889 (1973).
9. A. T. Ward, A. Damjanovic, E. Gray, and M. O'Jea, *This Journal,* **123,** 1599 (1976).
10. J. L. Ord and F. C. Ho, *ibid.*, **118,** 46 (1971).
11. A. Damjanovic and L.-S. R. Yeh, *ibid.*, **126,** 555 (1979).
12. A. Damjanovic, L.-S. R. Yeh, and J. F. Wolf, *ibid.*, **127,** 874 (1980).
13. A. Damjanovic, L.-S. R. Yeh, and J. F. Wolf, *ibid.*, **127,** 1949 (1980)
14. A. Damjanovic, L.-S. R. Yeh, and J. F. Wolf, **129,** 55 (1982).
15. S. Trasatti, *J. Electroanal. Chem.*, **52,** 313 (1974).
16. P. Delahay, in "Double Layer and Electrode Kinetics," pp. 156, 198, Interscience Publishers (1966).
17. S. Trasatti, *J. Electroanal. Chem.*, **52,** 34 (1974).
18. D. B. Sepa, M. V. Vojnovic, Lj. M. Vracar, and A. Damjanovic, Submitted to *Electrochim. Acta.*
19. K. I. Rozenthal and V. I. Veselovskii, *Dolk. Akad. Nauk. USSR,* **111,** 647 (1956).
20. J. O'M. Bockris and T. Otagawa, *J. Phys. Chem.*, **87,** 2960 (1983).
21. B. E. Conway and P. Bourgault, *Can. J. Chem.*, **37,** 292 (1959).
22. A. Damjanovic, J. F. Wolf, and S. L. Soled, In preparation.
23. D. Doblhofer, M. Metikos, Z. Ogumi, and H. Gerischer, *Ber Bensenges. Phys. Chem.*, **82,** 1046 (1978).

Relaxation Spectrum Analysis of Galvanostatic Oxidation of Silver Electrodes

Maria Hepel* and Micha Tomkiewicz*

Department of Physics, Brooklyn College of CUNY, Brooklyn, New York 11210

ABSTRACT

The frequency dispersion of the impedance of the silver electrode was measured during galvanostatic charging and discharging over the frequency range of 1-1.3 × 10^7 Hz. Prior work has indicated that the high frequency peak of the imaginary part originates from a response of a pure dielectricum with the properties of the Ag_2O layer from which the resistance and capacitance of the layer can be evaluated. In this paper, these two parameters are monitored as a function of the state of charge of the electrode during galvanostatic charging. Two regions on the galvanostatic plateau are detected which correspond to the formation of AgO during the charging of a smooth silver electrode. Each region corresponds to a different mechanism for formation of AgO: one directly from oxidation of Ag_2O; the second without Ag_2O as a precursor. Some of the charge during this stage is used for the formation of new Ag_2O. All this takes place with almost no detectable change in the measured electrode potential.

In a previous publication (1), we have demonstrated that, by using the technique of relaxation spectrum analysis to interpret the frequency dispersion of the impedance of charged silver electrodes, one can separately monitor the evolution of the two principal oxides that are involved in the process: Ag_2O and AgO. We have shown that, as soon as the insulating Ag_2O layer is covered with the considerably more conducting AgO, the system can be characterized as a parallel plate capacitor in which Ag_2O behaves as a pure dielectricum with a frequency-independent dielectric constant. It has been shown that, under potentiostatic conditions, even when the electrode potential is increased to values at which AgO is formed, a significant fraction of the charge is used to increase the thickness of the Ag_2O layer.

This paper is, to a degree, a continuation of that work, but the investigation here is centered around the galvanostatic charging and discharging of the silver electrode, which might make it more relevant for the understanding and monitoring of the state of charge of the silver electrode.

A literature survey of the silver electrode, with particular emphasis on characterization by impedance measurements and references that describe the technique of relaxation spectrum analysis is given in Ref. (1). Additional, pertinent, references that came to our attention since then are given in (2, 3).

*Electrochemical Society Active Member.

Experimental

The electrochemical cell and the experimental setup for impedance measurements were similar to the one described elsewhere (1). The counterelectrode for the impedance measurements was made from a large graphite cylinder. A double-junction saturated (KC1) silver/silver chloride with 1*M* KNO_3 external solution was used as a reference electrode. The silver working electrodes were prepared from silver rods (Johnson-Matthey, 99.99%) pressed into a Teflon holder. The exposed area of the electrodes was 0.385 cm^2.

All chemicals were of analytical grade. The deionized water (18 MΩ) was distilled from a Mili-Q purification system.

Procedure.—The polycrystalline silver electrodes were polished to a mirror-like finish using 0.03 μm alumina powder. The surface was subsequently degreased in acetone and propyl alcohol, etched in dilute HNO_3 solution, rinsed in deionized water, and dried in air. The electrodes were conditioned at a constant potential of $U = -0.5$V *vs.* Ag/